



## Effective Image Restoration of SAR Images

---

Vaishnavi Pillalamarri

EasyChair preprints are intended for rapid dissemination of research results and are integrated with the rest of EasyChair.

October 20, 2021

# EFFECTIVE IMAGE RESTORATION APPROACHES FOR SAR IMAGES

VAISHNAVI PILLALAMARRI

vaishnu.p.0207@gmail.com

## ABSTRACT

Landsat 7 Enhanced Thematic Mapper Plus satellite images presents an important datasource for many applications related to remote sensing. However, a component called Scan Line Corrector failure has seriously limited the scientific applications of ETM+ data since SLC failed permanently on May 31,2003 resulting in about 22% of the image data missing. An effective image restoration method is proposed to fill the missing information in the satellite images. The method is pre-processed by image resize, image enhancement and Gaussian filtering. The segmentation of satellite images are performed using Simple Linear Iterative Clustering to find the SLIC Super pixels and a dynamic clustering algorithm namely Regionalization with Dynamically Constrained Agglomerative Clustering and Partitioning algorithm to find the image Segments. The Boundary Reconstruction is performed using Edge Matching to find the area of the missing region and the matrix completion is used to fill the gaps of the satellite images using the Accelerated Proximal Gradient Line algorithm. The Landsat 8 Real images are compared with Landsat 7 Satellite images using the performance metrics namely Peak Signal to Noise Ratio and Root Mean Square Error to evaluate the quality and the errorrate of the satellite images. The Results show the capability to predict the missing value accurately in terms of quality, time without need of external information.

**Keywords-** Gap filling, Landsat 7 Enhanced Thematic Mapper Plus, Matrix Completion, Scan Line Corrector, segmentation, remote sensing.

## INTRODUCTION

Recovery of missing data in the satellite image is indispensable when the image acquired has been damaged by information

gaps provided by sensor failure. On average, about 22% of the total image is missing pixels in each scene. In addition, the areas of missing pixels are not identical across all multispectral bands and filling the missing region methods have been proposed by different research scholars in the field on remote sensing field.

Sina Ghassemi et.al [7] proposed an Adapting Robust Features for Satellite Image Segmentation on Heterogeneous Data Sets using a convolutional encoder–decoder network able to learn visual representations of increasing semantic level as its depth increases, allowing it to generalize over a wider range of satellite images. Yi et al. [18] proposed deriving the initial oversegmentation result of HSRI using an edge-embedded marker-based WT segmentation algorithm.

The above methods show the image segmentation the traditional pixel-based image segmentation algorithms, such as the WT algorithm, the RG algorithm, and the graph-based image segmentation algorithm. However, the WT algorithm is sensitive to the image noises. The RG algorithm does not adhere well to image boundaries. The graph-based image segmentation algorithm is inefficient. Thus, oversegmentation is not efficient and accurate to obtain the results. The training is done on heterogeneous Dataset and test samples are captured from the same city by the same satellite.

## III. Workflow

### 3.1 FILLING GAPS IN LANDSAT 7 SATELLITE IMAGES

The proposed method to fill the missing information in the satellite image without any spatial constraint applied on the neighbourhood of missing pixels. This is formulated by Segmenting the image of superpixels using SLIC to get SLIC Superpixels and a dynamic Clustering

using REDCAP to get image segments. Edge matching is performed using two edge couple on both sides of the information must be similar and magnitude of the local gradient must be similar and edges must keep one side inside region and other outside damaged region so they can interact with each other. The matrix completion is used for filling gaps is achieved by APGL. The results are compared using Landsat 7 Synthetic images and Landsat 8 Real images.

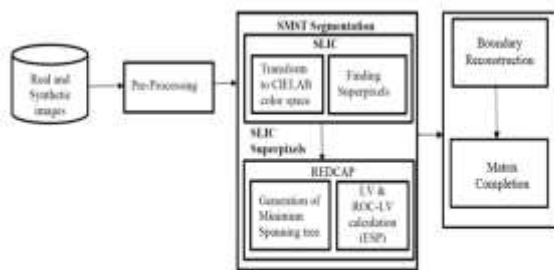


Fig 3.1 Overall Block Diagram of Image Restoration System

In Figure 3.1 explains about the overall Block Diagram of image Restoration System. The Dataset consist of Real and Synthetic Images is Preprocessed by Image Resize, Image Enhancement and Gaussian Filtering. The preprocessed satellite image is segmented using SMST Segmentation. The SLIC and REDCAP algorithm is used for clustering and regionalizing the satellite image. The Boundary Reconstruction is performed using Edge Matching Algorithm and Matrix Completion used APGL algorithm to fill the gaps.

### 3.2 SUPERPIXEL BASED SEGMENTATION

An Upgradation of K-means clustering algorithm is the Simple Linear Clustering Algorithm. This is used for efficiently generate Superpixels, where the image blocks are composed of adjacent pixels with a similar texture, color, brightness. The color image is converted from an RGB color space to a CIE LAB color space. A pixels color is represented in the CIE LAB color space. Image pixels are clustered to

generate Superpixels.

#### //Initialization

Initialize cluster center

$C_k = [l_k, a_k, b_k, x_k, y_k]$  by sampling pixels at regular grid steps  
Move Cluster Center to the lowest gradient position in a 3x3 neighborhood.

Set label  $(i) = -1$  for each pixel  $i$ .

Set distance  $(i) = \infty$  for each pixel  $i$ .

#### //Assignment

for each cluster center  $C_k$  do

for each pixel  $i$  in a  $2S \times 2S$  region around  $C_k$  do

compute the distance between  $C_k$  and  $i$ .

if  $D < d(i)$  then

Set  $(i) = D$  Set

$l(i) = k$

end if

end for

end for

#### //Update

Continue till new Cluster

Compute residual error  $E$

Until  $E \leq \text{threshold}$

The first step is initialization step where every pixel are placed on a regular grid. The pixel centers are moved to the seed locations corresponding to the lowest gradient position. In the assignment step, each pixel is clubbed with the nearest cluster center. The final step is the update step where each pixel is associated with the nearest cluster and updates the cluster. The assignment and update step is performed until the error converges.

$$d_c = \sqrt{(l_j - l_i)^2 + (a_j - a_i)^2 + (b_j - b_i)^2}$$

$$d_s = \sqrt{(x_j - x_i)^2 + (y_j - y_i)^2}$$

$$D' = \sqrt{\left(\frac{d_c}{c}\right)^2 + \left(\frac{d_s}{N_s}\right)^2}$$

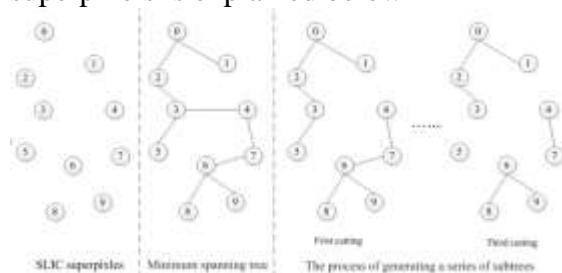


Fig 3.1 Output of SLIC

### 3.3 DYNAMIC REGION CLUSTERING

REDCAP algorithm is a dynamic region Clustering Algorithm. This was proposed by GUO[3]. The algorithm can make use of the attribute difference and adjacency relationship among different regions to merge regions. Pixel level classification is performed on very high resolution satellite images.

Regionalization is the process of dividing large set of spatial objects into a number of spatially contiguous regions which is normally a homogeneity or heterogeneity measure of the derived regions. It is done by using Full Order CLK Rule. Full Order CLK Rule is it need a matrix to keep the distance among existing clusters. The input which is the SLIC Superpixels undergoing REDCAP algorithms yields a set of image Segments. The process of merging the superpixels is explained below



The minimum spanning tree is divided according to the number of divisions. In the dividing process, the Superpixels included in the subtree are used for calculating the LV value. The ROC-LV is calculated with respect to LV values.

The mean value of standard deviation of spectral attribute of the pixels with in the window is calculated using LV. Accessing the dynamic LV from one object level to another is called ROC-LV calculated and plotted on ESP tool.

$$LV = \frac{1}{N} \sum_{r=1}^N \sqrt{\frac{1}{n_r} \sum_{j=1}^d \sum_{i=1}^{n_i} (x_{rj} - \bar{x}_{rj})^2}$$

According to the dynamic LV from one object level to another is a measurement called ROC-LV calculated and plotted using

ESP tool.

$$\left[ \frac{L_N - L_{N+1}}{L_{N+1}} \right] \times 100$$

where N is the set number of image segments, that is the number of subtrees. d is the number of attributes of the superpixel. nr is the number of superpixels in the subtree. xri j is the attribute j of the label i superpixel in the label r subtree.  $\bar{x}_{rj}$  is the mean value of attribute j of all superpixels in the subtree. LN is the LV value corresponding to the number of image segments N.

#### ALGORITHM

- STEP 1:** Take SLIC Superpixels as input.
- STEP 2:** Perform multiresolution segmentation on the SLIC Superpixels by following Full Order CLK Rule.
- STEP 3:** In the process of merging superpixels, the minimum spanning tree connecting all the superpixels is generated.
- STEP 4:** Then, the minimum spanning tree is divided according to the initial number of divisions.
- STEP 5:** Calculate the Local Variance (LV) and Region of Local Variance (ROC-LV) using ESP tool.

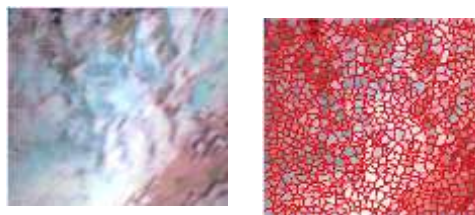


Fig 3.2 Output of REDCAP

### 3.4 EDGE MATCHING BASED ON MISSING REGION

Texture similarity and intensity of that area are essential for solving most the edge matching image inpainting problems. A proposed a novel image inpainting algorithm that is capable of producing the underlying textural details [20] and measure the smoothing pixel intensity in order to achieve natural-looking inpainted images.

Boundary Reconstruction [1] is used to get

the image structure of the missed area. The boundary of the segments resulting from the segmentation step, the edge features are then extracted for each edge. They include the intensity on both sides of the edge, and the magnitude of the local gradient is similar along the edge. This information is used for finding the image structures of the missed area. Thus the image structure of the missed area is found.

### Types of Edges:

**Matched edge** – It consist of the edges which are closely related to each other. The grey value of the point in the radian is given as:

$$\lambda^{pi} = \frac{W_1 \lambda^{P1} + W_2 \lambda^{P2}}{W_1 + W_2}$$

**Coupled edge** – It consist of the edges which are moderately related to each other. The grey value of the point in the radian is given as:

$$\lambda^E = \frac{W_1^c \lambda^{P1} + W_2^c \lambda^{P2}}{W_1^c + W_2^c}$$

**Single edge** – It consist of edges which are unrelated to each other. the Euclidian distance between point E and pi ( $i \in 1, 2$ )

$$\lambda^{pi} = \frac{W_1^b \lambda^{P1} + W_E^b \lambda^{P2}}{W_1^b + W_E^b}$$

$$\lambda^{pi} = \frac{W_1^c \lambda^{P1} + W_E^c \lambda^{P2}}{W_1^c + W_E^c}$$

### ALGORITHM FOR EDGE MATCHING

**STEP 1:** Find the image structure of the missing region.

**STEP 2:** The edge features are then extracted for each edge which include the intensity on both sides of the edge, and the magnitude of the local gradient along the edge.

**STEP 3:** Based on the missing pixel region check which edge is matching either the Matched edge, Coupled edge or the Single edge.

**STEP 4:** Perform the matching and check which edges which are matching to perform the reconstruction.

**STEP 5:** If the output is black for any of the above mentioned edges then it indicates there

is no match.



Fig 3.3 Output of Edge Matching based on Missing Region

The figure 3.3 describes the output of Edge Matching. When comparing with input image and image segments which is the output of REDCAP, there is no relation in matched edge and in Coupled edge where edges are moderately related and single edge, where the edges are totally unrelated. For the single edge, the restoration method is same as the coupled edge. The single edge will get interconnected with the edge to be restored well. If the single edge is not interconnecting with any other edge, the edge interacts with the boundary of the mask, and then connects them with an arc, where its curvatures are all similar to the connected edges.

### 3.5 FILLING MISSING GAPS

The proposed restoring method to fill the region, taking into account the physical characteristics and geometric features of the ground coverage of the missing strips is done through through Matrix Completion.

The method for reconstructing and identifying the structure of the boundary of the missed region is performed using matrix completion. The completion method is used to fill the rest of the missing information in the damaged region. The Matrix Completion can be formulated using Accelerated Proximal Gradient Line Algorithm [1]. The APGL is originated in work by Nesterov in the 1980s and it improves convergence.

### ALGORITHM FOR FILLING MISSING GAPS

Input: tolerance  $\epsilon$ , matrix  $M_n$

1. Initialize  $t_1 = 1, X_1 = M_{ij}, Y_1 = X_1$

2. Repeat

$$X_{k+1} = \operatorname{argmin} \|X\|_1 + \frac{1}{2t_k} \|X - (Y_k - t_k \Delta f(Y_k))\|_F^2$$

$$Y_{k+1} = X_{k+1} + \frac{t_k - 1}{t_{k+1}} (X_{k+1} - X_k)$$

$$t_{k+1} = \frac{1 + \sqrt{1 + 4t_k^2}}{2}$$

Until convergence:  $\|X_{k+1} - X_k\|_F \leq \epsilon$

The Accelerated Proximal Gradient Line (APGL) method uses the accelerate the convergence of Proximal Gradient. Instead of making quadratic approximation around  $X_k$ , APGL makes the approximation at another point  $Y_k$ , which is a linear combination of  $X_k$  and  $X_{k-1}$ . This modification will give a convergence rate of  $O(1/k^2)$ .



Fig 3.4 Output of Filling Missing Gaps

## DATASET DESCRIPTION

Dataset consist of both Synthetic and Real images. Synthetic Images are color images used in three channels[Red, Green, Blue]. The real image is a Landsat 8 satellite image downloaded from united states geological survey for earth resource observation and science center with path:200 and row:36. It is located in north of Africa. The images aredownloaded with Latitude value and Longitude value of (32.71,-6.04) respectively. TheDataset has been downloaded from <https://earthexplorer.usgs.gov/>.

## IV. RESULTS

### 4.1 PEAK SIGNAL TO NOISE RATIO(PSNR)

This computes the term peak signal-to-noise ratio (PSNR) is an expression for the ratiobetween the maximum possible value (power) of a signal and the power of distorting noise that affects the quality of its representation.

$$\text{PSNR} = 10 \log_{10} \left( \frac{R^2}{\text{MSF}} \right)$$

### 4.2 ROOT MEAN SQUARED ERROR (RMSE)

It is the standard deviation of the residuals. Residuals are a measure of how far fromthe regression line data points are measured. This computes the root of the expected squared error between the predicted time values and the ground truth:


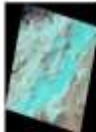

$$\text{RMSE} = \sqrt{\frac{1}{N} \sum_{i=1}^N (t_i - \hat{t}_i)^2}$$

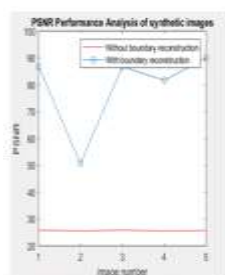
The table 5.1 and 5.2 describes about the values of both synthetic images and Real images. The tabular values are plotted between the PSNR with and without Boundary Reconstruction.

Table 5.1 Values for Synthetic Images

Synthetic Image	PSNR without Boundary Reconstruction	PSNR with Boundary Reconstruction	RMSE without Boundary Reconstruction	RMSE with Boundary Reconstruction
	R=25.6082	R=91.55	R=180.16	R=4.57
	G=25.61	G=54.52	G=179.90	G=0.23
	B=25.6086	B=53.08	B=180.14	B=0.32
	R=25.60	R=50.75	R=180.10	R=0.55
	G=25.62	G=39.17	G=179.61	G=7.93
	B=25.61	B=47.25	B=180.07	B=1.23
	R=25.87	R=86.78	R=169.59	R=1.37
	G=25.69	G=67.30	G=176.75	G=0.01
	B=25.65	B=62.94	B=178.16	B=0.03
	R=25.60	R=81.70	R=180.14	R=4.42
	G=25.62	G=50.06	G=179.62	G=0.64
	B=25.61	B=54.40	B=179.82	B=0.23

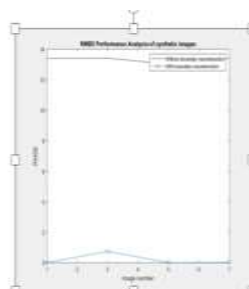
**Table 5.2** Values for Real Images

Real Image	PSNR with Boundary Reconstruction	PSNR without Boundary Reconstruction	RMSE without Boundary Reconstruction	RMSE with Boundary Reconstruction
	R=25.74 G=25.733 B=25.730	R=49.00 G=49.38 B=49.63	R=174.64 G=175.04 B=175.16	R=0.00 G=0.75 B=0.71
	R=25.66 G=25.655 B=25.654	R=48.77 G=32.31 B=33.72	R=177.99 G=178.24 B=178.21	R=0.86 G=38.42 B=27.76
	R=25.66 G=25.6598 B=25.6593	R=90.04 G=93.31 B=88.37	R=177.95 G=178.03 B=178.05	R=6.48 G=3.05 B=9.53

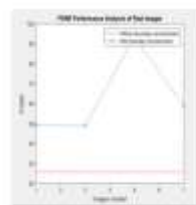


**PSNR Performance analysis for Synthetic Images**

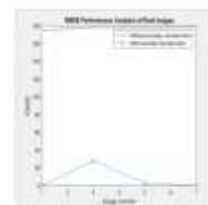
The graph 5.3 is plotted between image number and PSNR. The graph indicated that PSNR for synthetic images using with Boundary Reconstruction is high when compared to real images. The graph 5.4 is plotted between image number and RMSE. The graph indicates that error rate is less for with Boundary Reconstruction.



**RMSE Performance analysis for Real Images**



**Fig 5.5** PSNR Performance Analysis Real images



**Fig 5.6** RMSE Performance Analysis for Real Image

In figure 5.5 the graph is plotted between image number and PSNR. The graph indicated that PSNR for Real images using with Boundary Reconstruction is less and in figure 5.6 error rate is high when compared to Synthetic images. Thus for Synthetic images the Quality of the image is high and error rate is low.

## CONCLUSION

A novel approach for filling gaps based on Segmentation and matrix completion reinforced by edges restoration. The problem of restoring and filling the unscanned gaps in Landsat 7 SLC-off ETM+ images was resolved accurately and without need of an external information. Segmentation is done using SLIC for detecting the Superpixels and a dynamic clustering algorithm namely REDCAP algorithm is used for getting the image segments. The application of matrix completion method is based on low-rank approximation using Accelerated Proximal Gradient Line algorithm (APGL) used for filling the gaps in satellite images. Experiments are done on both synthetic and real satellite images and measure the Quality of the image using Peak Signal to Noise Ratio (PSNR) and Root Mean Square Error (RMSE). The results show that for the reconstructed satellite images the Quality of the image is high and the error rate is low when comparing with Landsat 7 synthetic image with Landsat 8 real image.

## FUTURE WORK

The problem of damaged area is taken into study due to the presence of cloud and shadow region in satellite image which is a very large damaged region. Our

perspective is to clear the region and study the information.

## REFERENCES

- [1] Salma El Fellah, Mohammed Rziza, Mohamed El Haziti. An Efficient Approach for Filling Gaps in Landsat 7 Satellite Images. *GRSL* 2017; 14:162-66.
- [2] Radhakrishna Achanta, Appu Shaji, Kevin Smith, Aurelien Lucchi, Pascal Fua, and Sabine S`usstrunk. SLIC Super Pixels Compared to State-of-the-art Super Pixel Methods. *Journal of Latex Class Files* 2011;34:11 2274-2282.
- [3] D.Guo. Regionalization with dynamically constrained agglomerative clustering and partitioning. *International Journal of Geographical Information Science* 2007; 22:7 80-823.
- [4] Mai Quyen Pham , Pascal Lacroix, Marie Pierre Doin. Sparsity Optimization Method for Slow-Moving Landslides Detection in Satellite Image Time-Series. *GRSL* 2019 ; 57:3 2133-2144.
- [5] Yangyang Li , Cheng Peng, Yanqiao Chen , Licheng Jiao, Linhao Zhou, Ronghua Shang. A Deep Learning Method for Change Detection in Synthetic Aperture Radar Images. *GRSL* 2019; 57:8 5751-5763.
- [6] Kalamraju Mounika , Sheeba Rani J, Govindan Kutty , Sai Subrahmanyam R. K. Gorthi. Consistent Robust and Recursive Estimation of Atmospheric Motion Vectors From Satellite Images. *GRSL* 2019; 57:3 1538-1544.
- [7] Huihui Song, Bo Huang, Kaihua Zhang. Shadow Detection and Reconstruction in High-Resolution Satellite Images via Morphological Filtering and Example-Based Learning. *GRSL* 2014; 52:5 2545 – 2554.
- [8] Chao-Hung Lin, Po-Hung Tsai, Kang-Hua Lai, Jyun-Yuan Chen. Cloud Removal from Multitemporal Satellite Images Using Information Cloning. *GRSL* 2013 ;51:1 232- 241.
- [9] K.C. Toh and S.Yun . An accelerated proximal gradient algorithm for nuclear norm regularized least squares problems. *Pacific J. Optim* 2010; 6:3 615-640.
- [10] L. Ashok Kumar, M.R. Ebenezar Jebarani. A Comprehensive Review on Speckle Denoising Techniques in Satellite Images. *ICCSP* 2019 0245-0248.
- [11] Chen Yi, Yong-Qiang Zhao. Spectral Super Resolution for multispectral image based on Spectral improvement strategy and spatial Preservation Strategy. *GRSL* 2019; 57:11 9010-9024.
- [12] Dawa Derksen , Jordi Inglada, and Julien Michel. Scaling Up SLIC Superpixels Using a Tile-Based Approach. *GRSL* 2019; 57:5 3073-3085.
- [13] Sina Ghassemi , Attilio Fianrotti, Member, Gianluca Francini, and Enrico Magli. Learning and Adapting Robust Features for Satellite Image Segmentation on Heterogeneous Data Sets . *GRSL* 2019 57:9 6517 – 6529.
- [14] Liang Yan , Bin Fan , Hongmin Liu , Chunlei Huo , Shiming Xiang and Chunhong Pan. Triplet Adversarial Domain Adaptation for Pixel-Level Classification of VHR Remote Sensing Images. *GRSL* 2019 1-16.
- [15] Mi Wang, Zhipeng Dong, Yufeng Cheng, and Deren Li. Optimal Segmentation of High-Resolution Remote Sensing Image by Combining Superpixels With the Minimum Spanning Tree. *GRSL* 2018 56:1 228-238.
- [16] Jiaqing Miao , Xiaobing Zhou , Ting-Zhu Huang , Tingbing Zhang, and Zhaoming Zhou.
- [17] A Novel Inpainting Algorithm for Recovering Landsat-7 ETM+ SLC-OFF Images Based on the Low-Rank Approximate Regularization Method of Dictionary Learning With Nonlocal and Nonconvex Models. *GRSL* 2019 57:9 6741-6754.